Emergent Materials (2025) 8:6509–6521
https://doi.org/10.1007/s42247-025-01087-8

ORIGINAL ARTICLE

Enzymatic etching of PLA/hydroxyapatite scaffolds for improved cell adhesion: surface modification and homogeneity

Attila Ur[1,2] · Dóra Plachi[1,2] · Viktória Varga[3] · István Hornyák[3] · Loránd Románszki[1] · Miroslav Slouf[4] · Nóra Hegyesi[1,2] · János Móczó[1,2] · Dorottya Kardos[1,2] · Dóra Tátraaljai[1,2] · Béla Pukánszky[1,2]

Received: 17 February 2025 / Accepted: 1 April 2025 / Published online: 21 April 2025

Abstract
Nanosized hydroxyapatite (HAP) particles were produced by precipitation, and poly(lactic acid) (PLA) composites containing 5 wt% of the nano HAP were prepared in an internal mixer to prepare scaffold materials. The nanoparticles aggregated without surface modification. Applying stearic acid coating on HAP particles decreased aggregation and improved homogeneity. The extent of coating must be optimized, the amount of stearic acid needed for monolayer coverage is around 4 wt% for the HAP prepared. A polymer layer always forms on the surface of PLA products during the melt processing of PLA/HAP composites, HAP particles are not available to help bone regeneration. The surface layer was removed successfully by enzymatic etching. The amount of removed PLA polymer depended quite strongly on the extent of surface coating. Etching disclosed the HAP particles, which led to increased surface roughness and decreased wettability, but this did not influence the adhesion of cells on the surface. Scaffolds could be prepared successfully by 3D printing from the composites containing the coated particles, which, in all probability, can be successfully used for bone regeneration.

Keywords Nanofiller · Precipitation · Proteinase K · Stearic acid · Monolayer coverage · AFM · Surface roughness · Molecular mobility · 3D printing

1 Introduction

Tissue engineering is an important discipline in modern medicine, improving the quality of life considerably. The replacement of damaged or dead tissues accelerates recovery and reduces the time of convalescence [1]. The replacement of bones has a long history, starting in the 17th century. The use of real bones, i.e. autograft, allograft, or xenograft replacement, has serious drawbacks; thus, currently, mostly artificial bone materials are used in surgery [2, 3]. These replacement scaffolds are frequently prepared from biopolymers, poly(lactic acid) (PLA), poly(hydroxyl alkanoate) (PHA), polycaprolactone (PCL) [4, 5]. However, the successful use of scaffolds has many requirements, including biological, medical, or engineering aspects. Thus the polymers are often modified by blending [6], the addition of fillers [7, 8], reinforcements [9], various additives [10, 11], or surface modification [12–14].

The biopolymer produced and used in the largest quantity today is PLA [15]. It has numerous advantages but also several drawbacks. PLA is utilized mostly as packaging material [16], but engineering parts are also prepared from it in increasing quantities [17]. In medicine, PLA is used in tissue engineering, drug release systems, medical devices and prostheses, surgical tools, etc. [18]. Scaffolds are often prepared from PLA by 3D printing [19, 20]. The devices

✉ Dóra Tátraaljai
tatraaljai.dora@ttk.hu

1 Institute of Materials and Environmental Chemistry, HUN-REN Research Centre for Natural Sciences, Magyar tudósok körútja 2., Budapest H-1117, Hungary

2 Laboratory of Plastics and Rubber Technology, Department of Physical Chemistry and Materials Science, Faculty of Chemical Technology and Biotechnology, Budapest University of Technology and Economics, Műegyetem rkp. 3., Budapest H-1111, Hungary

3 Institute of Translational Medicine, Semmelweis University, Tűzoltó utca 37-47, Budapest H-1094, Hungary

4 Institute of Macromolecular Chemistry, Czech Academy of Sciences, Heyrovskeho namesti 2, Praha 6 16206, Czech Republic

thus produced are biocompatible, biodegradable and possess good mechanical properties [20]. 3D printing offers enormous flexibility in manufacturing devices and allows the production of personalized replacements.

One of the modifications used to improve the biological and mechanical characteristics of PLA is the addition of hydroxyapatite [21–23]. Bones contain a large amount, approximately 70% of HAP; thus, their inclusion in a biopolymer scaffold facilitates cell adhesion, proliferation and differentiation and minimizes the danger of infection or the rejection of the scaffold [24]. Accordingly, numerous papers have been published on PLA/HAP composites focusing on many aspects of scaffold preparation, mechanical properties, and questions related to biology [25–27]. The amount of HAP in the composites varies from a few percent up to 50 wt% or more in the form of nanometer [28, 29] or micron-sized particles [22, 30]. The increased amount of HAP is claimed to improve the bioactivity of the scaffold. Nanoparticles are more beneficial since their large specific surface area reinforces the polymer to a larger extent and offers a larger surface for cell adhesion and proliferation.

Unfortunately, one encounters several difficulties during the preparation of PLA/HAP nanocomposites, which are rarely discussed in current literature [29]. The distribution of any nanofillers is quite difficult in polymers, the small particles tend to form larger aggregates [31]. The benefits of the nanometer size are lost with aggregation. Moreover, several difficulties might occur during the processing of the material, and its mechanical properties also deteriorate considerably; both strength and fracture resistance decrease below acceptable levels [27]. Homogeneity can be improved by various means, but the most convenient and often used approach is the surface coating of the filler with a surfactant [26, 27]. Although surface modification improves homogeneity, it might influence biological activity and deteriorate cell adhesion.

Another problem that is rarely discussed is the fact that particulate-filled materials, including PLA/HAP nanocomposites, are always covered by a skin layer of the polymer, irrespective of the manufacturing technology. Inorganic fillers, like HAP, have large surface energies thus, the polymer with much smaller surface tension migrates to the surface to decrease interfacial tension. Consequently, the HAP particles of the scaffold are not in direct contact with the living tissues and cannot exert their beneficial effect on cell adhesion, differentiation, and proliferation completely. In order to access the HAP particles and accelerate healing, the polymer surface layer should be etched off to the necessary extent.

Various approaches can be used for the removal of the polymer surface layer. The degradation of the layer leaves HAP particles embedded into the polymer behind. Plasma is often used to modify the surface of polymers, including PLA/HAP scaffolds [32, 33]. Depending on the composition of the plasma and treatment conditions, various polar functional groups form on the surface of the polymer and a layer is removed as well. However, the thickness of this layer is small even in the case of extremely intensive treatment [34] and does not guarantee that a sufficient amount of HAP emerges on the surface. Another approach might be the chemical or enzymatic etching of the scaffold. Acidic [35] or alkali [36] treatments are well-known methods to increase the surface roughness of a scaffold, but PLA can be degraded efficiently with enzymes as well [37], degradation proceeds under benign conditions, and the thickness of the removed layer can be controlled quite easily. Although the biodegradation of PLA by microorganisms or enzymes is studied extensively [38–40], according to our knowledge, the method has never been used for the surface modification of PLA/HAP scaffolds.

Accordingly, the goal of the study was to check the possibility of etching the surface of PLA/HAP nanocomposites in order to make available the HAP surface for cell adhesion and proliferation. Nanosized HAP particles were prepared by a precipitation method, characterized, and surface-modified with stearic acid to various extents in order to assist homogenization. Composites were prepared in an internal mixer and subsequently compression molded into plates. The surface of composite specimens was etched in a buffer solution containing the enzyme, which catalyzes the degradation of PLA. The surface was characterized by various methods, including atomic force microscopy, contact angle measurements, and FTIR spectroscopy. The effect of etching and the surface modification of HAP were also checked by cell adhesion measurements.

2 Experimental

2.1 HAP synthesis

The nanosized HAP particles were prepared by precipitation from calcium nitrate tetrahydrate (99%, Molar Chemicals Ltd., Halásztelek, Hungary) and diammonium hydrogen phosphate (98%, Alfa Aesar, Karlsruhe Germany) according to a procedure published in the literature [41]. Calcium nitrate was dissolved in distilled water and heated to 80 °C. The hydrogen phosphate was also dissolved and added dropwise while the solution was stirred at 500 rpm. The pH of the solution was kept at 10 with ammonium hydroxide (25%, VWR International, Debrecen, Hungary), and the reaction ran for 6 h. Subsequently, the precipitated product was sedimented overnight, and then the watery phase was removed. The precipitate was washed and filtered. The

product obtained was dried at 105 °C, and then calcined at 700 °C. The calcined HAP was disintegrated in a ceramic mortar before composite preparation and/or surface coating.

2.2 Surface coating

5 g HAP was measured into a round bottom flask and then 200 ml 96% ethanol (Molar Chemicals Ltd., Halásztelek, Hungary) was poured on it. The necessary amount of stearic acid (StAc, 95%, Molar Chemicals Ltd., Halásztelek, Hungary) was added and then the suspension was stirred with an IKA T25 Ultra-Turrax mixer (IKA-Werke GmbH & Co. KG, Staufen im Breisgau, Germany) for 1 min at 25 000 rpm. The flask was placed into an oil bath and thermostated to 80 °C [42]. After 4 h of stirring at 1500 rpm, the contents were poured into a crystallization vessel, the ethanol was evaporated, and the product was ground in a braying mortar and stored for further use. HAP was treated with 2, 4, 6, 8 and 10 wt% stearic acid calculated for the amount of the filler.

2.3 Composite preparation

PLA (Ingeo 4032 D, Natureworks, Plymouth, MN, USA) was dried for 4 h at 90 °C before homogenization. The polymer and HAP were homogenized in a Brabender W 50 EH internal mixer (Brabender GmbH & Co. KG, Duisburg, Germany) at 190 °C and 50 rpm for 10 min. All composites contained the nanofiller at 5 wt%. The homogenized material was compression molded into 1 mm thick plates using an SRA 100 machine (Fontijne, Vlaardingen, The Netherlands). Discs with 55 mm diameter and 0.1 mm thickness were also compression molded for further investigations. Films and sheets were prepared at 190 °C and 5 min (3 min preheating and 2 min compression time).

2.4 Etching, enzymatic degradation

The etching of the samples was followed by the measurement of sample weight and the determination of the amount of the degradation product, lactic acid. Discs of 55 mm diameter and 100 µm thickness (approx 300 mg) were placed into vials containing 7.5 ml tris buffer containing 0.1 g/l Proteinase K from *Tritirachium album* (VWR International, Debrecen, Hungary). The tris buffer was prepared by dissolving 50 mmol tris(hydroxymethyl)aminomethane solution (tris, 99.5%, Molar Chemicals, Halásztelek, Hungary) in 900 ml distilled water then the pH of the solution was adjusted with the addition of HCl to 8.5, finally the solution was diluted to 1 l in a measuring flask. Etching was carried out at 40 °C for 24 h with continuous shaking.

The amount of lactic acid formed was determined by complexation with iron(III) chloride hexahydrate (min 99%, Honeywell, Charlotte, CA, USA) having an absorption maximum at 390 nm in the UV-Vis spectrum [43]. 75 µl degradation medium was added to 3 ml reagent solution (3 mg/ml) to form the complex. The background was recorded with 3 ml reagent and 75 µl buffer. Spectra were recorded using a Unicam UV-500 apparatus (Thermo Scientific, Haverhill, MA, USA) between 190 and 600 nm at 600 nm/min scan rate and 1 nm resolution in a quartz cuvette of 1 cm thickness.

2.5 Characterization

The structure of HAP nanoparticles was characterized by transmission electron microscopy (TEM) using a Tecnai G2 Spirit (FEI, Brno, Czech Republic) microscope, which was equipped with an energy dispersive spectrometer (EDX; Mahwah, NJ, USA). The sample for TEM microscopy was prepared by dispersing the HAP nanoparticles in ethanol (EtOH) first. Subsequently, a 4 µL droplet of the EtOH dispersion was deposited on a standard TEM copper grid covered with an electron-transparent carbon film. The excess of EtOH was removed by touching the bottom of the grid with a thin strip of filtering paper (this is an important step to minimize drying artifacts), and the sample was left to dry completely at ambient temperature. In TEM, the morphology of the nanoparticles was visualized by standard bright field imaging (TEM/BF), elemental composition was assessed by energy-dispersive spectroscopy (TEM/EDX), and crystal structure was verified by means of selected-area electron diffraction (TEM/SAED). The experimental electron diffraction pattern was processed by ProcessDiffraction [44] and compared with the theoretical powder X-ray diffraction pattern of hydroxyapatite that was calculated by PowderCell [45]. All TEM measurements were performed at the accelerating voltage of 120 kV.

The surface of the composite samples was studied by atomic force microscopy (AFM) before and after etching. AFM scans were performed at room temperature, using a Dimension 3100 AFM instrument equipped with a NanoScope IIIa controller (Digital Instruments/Veeco, Santa Barbara, CA, USA) at 512×512 pixel resolution. TM PPP-NCHR- 20 type silicon cantilever Nanosensors were used in the tapping mode. The cantilever was mounted at 10° with respect to the sample stage plane. The characteristics of the sensors were: thickness: 40 ± 1 µm; length: 125 ± 10 µm; width: 30 ± 7.5 µm; typical resonance frequency ~293 kHz; force constant: 10–130 N/m; aluminum-coated top; tip height: 10–15 µm; typical tip radius <7 nm; tip half cone angle along the cantilever axis: 10°. Scanned areas ranged from 2×2 to 100×100 μm^2. Scan rates were 0.1–0.5 Hz

(lines per second), corresponding to tip velocities ranging from 0.2 to 10 µm/s, depending on the scanned area. Both height and amplitude data were recorded. Off-line processing of the recorded raw data involved one or more of the following: 1st and 2nd order plane fit, 0th order flattening, and "erase scan lines" treatment. The roughness of sample surfaces was compared by the root mean square areal roughness parameter (S_q), defined as

$$S_q = \sqrt{\frac{\sum_{i=1}^{n} z_i^2}{n}} \quad (1)$$

where z_i is the height of the i^{th} measurement point, measured from the fitted mean plane, and n is the number of data points.

The specific surface area of the hydroxyapatite was determined by nitrogen adsorption using a Quantachrom Nova 2000 apparatus (Micrometics, Norcross, GA, USA). Samples were degassed at 200 °C in vacuum for 24 h before the measurement. The specific surface area was obtained from the Brunauer-Emmett-Teller (BET) model [46] using 0.162 nm^2 as the area occupied by one nitrogen molecule.

Wettability was characterized by the measurement of the contact angle of water on the surface of composite samples. A Ramé-Hart 100–00 equipment (Ramé-Hart Instrument Co., Succasunna, NJ, USA) was used for the determination of contact angle, the results were evaluated by the ImageJ software. Contact angles were determined 0.5–1 s after placing the droplet. Five parallel measurements were done on each sample.

The chemical composition of the samples and the result of etching were followed by Fourier transform infrared spectroscopy (FTIR). The measurements were done in the ATR mode using a Bruker Tensor 27 equipment (Bruker Optik GmbH, Leipzig, Germany). Five spectra were recorded from 4000 to 400 cm^{-1} at 16 scans with 2 cm^{-1} resolution on each sample.

Melting and crystallization characteristics, as well as the glass transition temperature of the samples, were determined using a Perkin Elmer DSC 8500 apparatus (Norwalk, CT, USA). Thermograms were recorded on 4–5 mg samples in two heating and a cooling run between 30 and 220 °C in a nitrogen atmosphere at 10 °C heating and cooling rates. DSC was also used for the determination of the surface coverage of HAP with stearic acid. The measurements were carried out using a Perkin Elmer DSC 7 apparatus (Norwalk, CT, USA) in oxygen atmosphere. 10 mg samples were heated from 30 to 450 °C at 10 °C/min heating rate to determine the total amount of stearic acid on the surface of the mineral as well as the melting of surplus StAc exceeding monolayer coverage.

2.6 Cell adhesion

Human bone marrow-derived mesenchymal stem cells (hBM-dMSCs) were cultured in T75 TC treated culture flasks in an incubator at 37 °C, 5% CO_2, and 95% humidity. The hBM-dMSCs were maintained in a stem cell medium: Dulbecco's modified Eagle's medium (DMEM) containing 4.5 g/L glucose and L-glutamine (Lonza, Basel, Switzerland) supplemented with 10% fetal bovine serum (FBS; EuroClone, Pero, Italy), 1% Penicillin–Streptomycin (Sigma-Aldrich, St. Louis, MO, USA), and 0.75 ng/mL basic fibroblast growth factor (Sigma-Aldrich, St. Louis, MO, USA). The culture medium was refreshed 3 times a week, and all cell culture procedures were carried out in a sterile laminar flow tissue culture hood. Circle plates with 5 mm diameter of the etched polymer samples were sterilized in absolute ethanol and placed into the wells of 96-well, ultra-low attachment plates in 100 µL of stem cell medium, and 30 000 hBM-dMSCs (4 passages) were seeded on each sample. The medium was refreshed every 2 days. On the seventh day, the viability of the seeded cells was measured using the Cell Proliferation Kit II (XTT; Roche, Mannheim, Germany), according to the instructions of the manufacturer.

3 Results and discussion

The results are presented in several sections. The preparation, characteristics, and coating of the HAP particles are presented first, followed by the results obtained on the enzymatic etching of the composites. The composition, morphology, and energetics of the etched surface are described in the next section. The results obtained in the cell adhesion experiments are discussed subsequently, followed by a general discussion of major questions and relevance in the final section of the paper.

3.1 HAP characterization, coating

Aggregation is a major problem in all particulate-filled and reinforced polymers, which becomes more severe as filler content increases. The problem is especially serious in the case of nanosized fillers and reinforcements. Accordingly, the proper characterization of the mineral is crucial for the understanding of its behavior and the interpretation of the properties of its composites. In this study, the prepared nanoparticles were characterized by TEM microscopy as summarized in Fig. 1. TEM/BF micrographs (Fig. 1a) documented that the precipitation method yielded nanosized particles with an average length of 113 nm and a diameter of 38 nm. The experimental TEM/SAED diffraction pattern (Fig. 1b) was converted to a 1D diffraction profile and

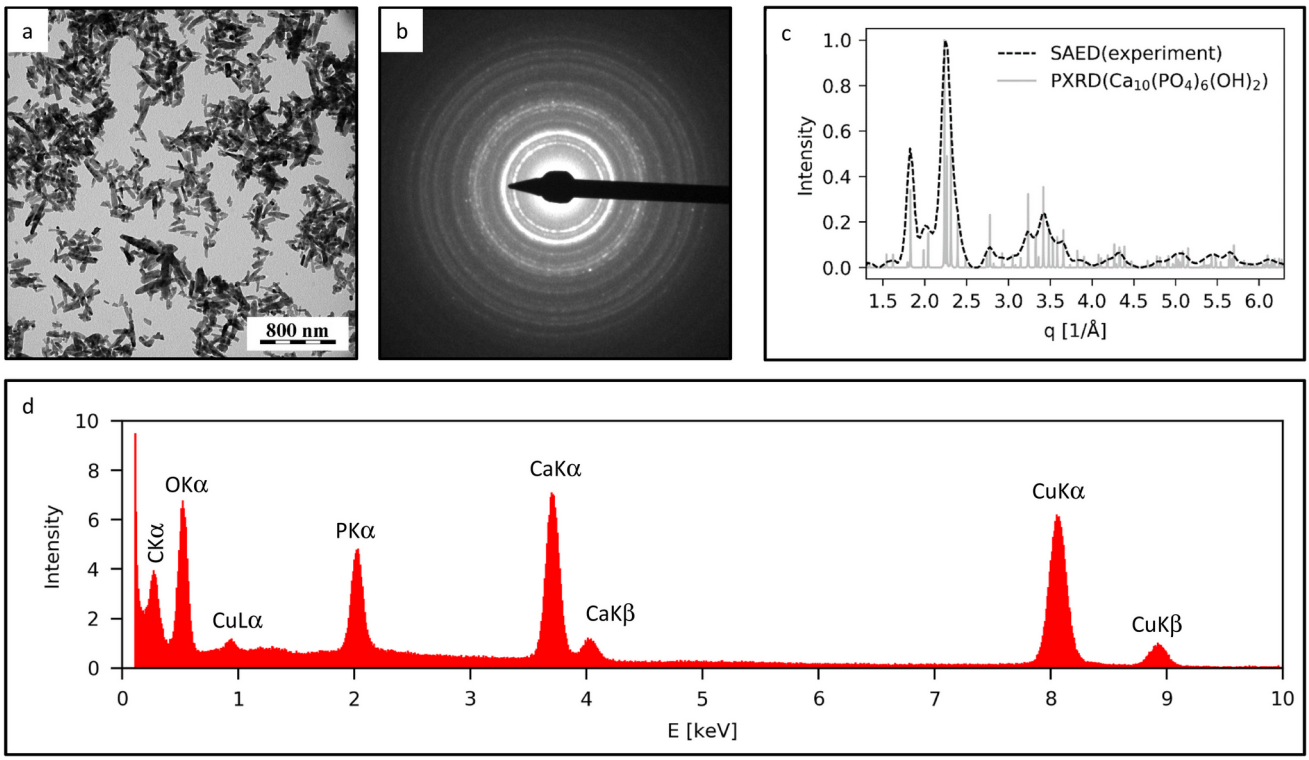

Fig. 1 TEM characterization of the HAP particles prepared by the precipitation method: (**a**) TEM/BF micrograph, (**b**) TEM/SAED diffraction pattern, (**c**) comparison of the experimental diffraction pattern (black dotted line) with the theoretically calculated powder X-ray diffraction pattern of hydroxyapatite (grey line), and (**d**) TEM/EDX spectrum of the nanoparticles that confirms their chemical composition

compared with a theoretically calculated powder X-ray diffraction pattern (PXRD) of hexagonal hydroxyapatite, $Ca_{10}(PO_4)_6(OH)_2$ (Fig. 1c). The good agreement between the experimental and theoretical diffraction patterns confirmed that the prepared nanoparticles are nanocrystalline HAP. The fact that the electron diffraction peaks are broader than the theoretically calculated PXRD diffraction peaks is typical for small nanoparticles observed by electron diffraction, as documented elsewhere [47, 48]. The TEM/EDX spectrum (Fig. 1d) showed just the peaks typical of hydroxyapatite (Ca, P, and O; hydrogen cannot be detected by EDX) and the supporting copper grid with electron-transparent carbon film (Cu and C) verifying that the prepared nanocrystals were chemically pure. The nanometer size is further confirmed by the large specific surface area of the filler, which is 42 m^2/g according to the BET method. The size and size distribution of the particles change during subsequent operations, i.e. surface coating, but the morphology of the primary particles determines their further behavior.

In order to prevent or at least decrease aggregation, the particles were coated with various amounts of stearic acid. Applying StAc as a surfactant for HAP nanoparticles helps to reach the required mechanical, thermal, and cytotoxicity properties for applications in PLA scaffolds [49]. However, the coating must always be carried out with the optimum amount of surfactant; an insufficient amount does not achieve the goal and decreases surface energy, while surplus coating agent may lead to migration, processing problems, and other difficulties [42], e.g., interference with cell adhesion and growth in our case. The optimum amount of coating agent is determined by the specific surface area of the filler and the orientation of the surfactant on the surface. A small amount of surfactant, up to monolayer coverage, adheres to the surface strongly, probably not by covalent [50] but by ionic bonds in our case, while excess surfactant forms multiple layers or dissolves in the polymer. Excess stearic acid crystallizes on the surface of HAP, and it can be detected by DSC by the measurements of its heat of fusion. This latter quantity is plotted against the extent of coating in Fig. 2. According to the figure, monolayer coverage is around 4 wt% stearic acid coating calculated for the amount of the filler.

The surface energy of fillers is usually large and decreases drastically as a result of coverage with an organic substance [51, 52]. Decreasing surface energy results in weaker particle/particle interactions leading to decreased aggregation. The effect is demonstrated well in Fig. 3. The compression-molded neat PLA disc is clear and transparent, while PLA filled with uncoated HAP contains large aggregates; the material is heterogeneous. Composites containing

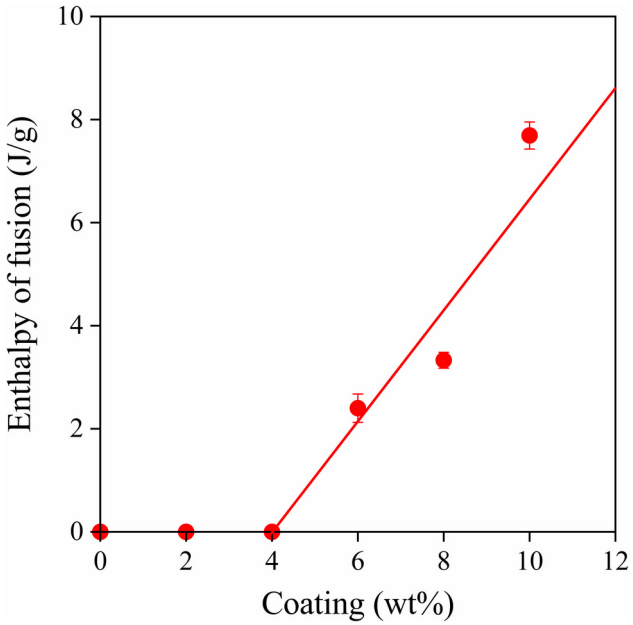

Fig. 2 Determination of the amount of strongly bonded stearic acid (monolayer coverage) by the measurement of the heat of fusion using DSC

coated particles are completely homogeneous, but the milky appearance indicates the presence of particles larger than nanometer size and/or the precipitation of surplus StAc surfactant in the polymer matrix. Both might influence etching and cell adhesion.

3.2 Enzymatic etching

Since the surface of thermoplastic composites is always covered by a skin layer, it should be removed to make HAP available for cell adhesion and proliferation. Etching can be done by various methods. One of the most often used approaches to modify the surface of polymers, including scaffolds, is plasma treatment [13]. However, the penetration depth of plasma is a few hundred nanometers at most, while the thickness of the skin layer is several microns. Accordingly, another technique must be used to remove this layer.

The enzymatic degradation of biopolymers is based on the catalytic effect of certain enzymes, which cleave the ester bonds of aliphatic polyesters [53]. The degradation proceeds in three steps: the adhesion of the enzyme on the surface of the substrate, degradation, which is often followed by the denaturation of the enzyme [54]. Degradation proceeds on the surface; enzymes are too large to diffuse into the bulk polymer, and thus, the method is ideal for surface etching. Using the results of previous studies [54], conditions were selected to remove several microns from the surface layer of the composites. Weight loss measured on the discs used in the study is plotted against the surface coating of HAP (Fig. 4). Degradation was followed by two techniques: by the direct measurement of weight and the detection of the lactic acid formed by complexation and UV-Vis spectrophotometry. The results of this latter approach were recalculated into weight loss in order to make the two methods comparable. As Fig. 4 shows, the two detection methods give practically the same results. We can also see that a considerable amount of PLA is removed from the surface of the discs, and the amount depends on the extent of HAP coating, which is somewhat surprising.

The variation in the amount of degraded PLA must be related to the changes in the structure of the composites and/or the effect of surplus stearic acid not bonded

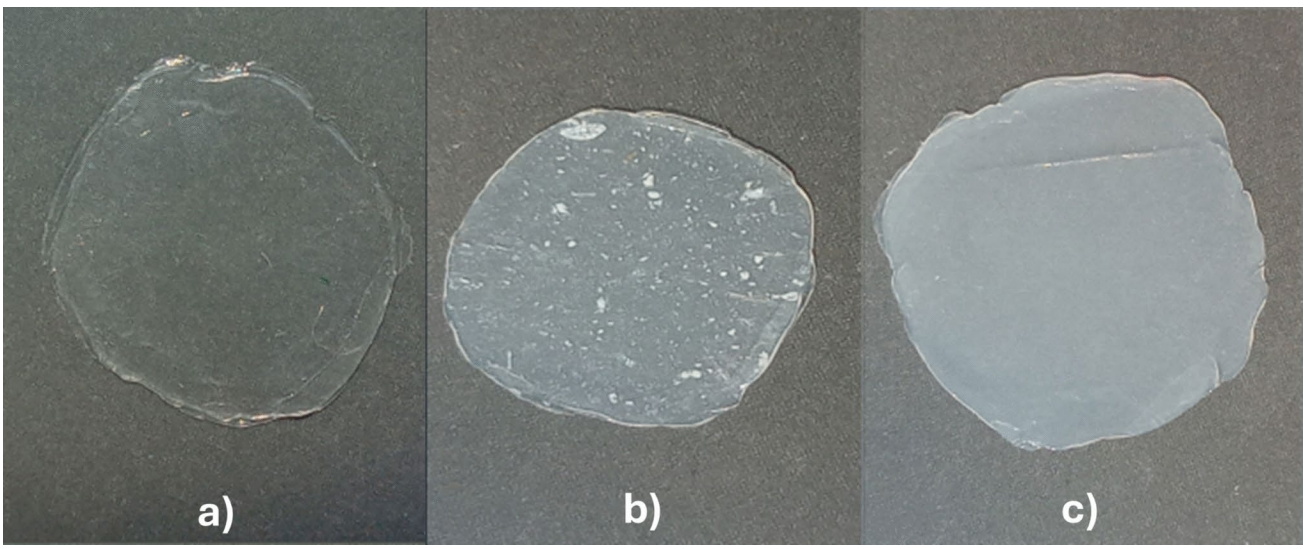

Fig. 3 Photos demonstrating the homogeneity of PLA composites prepared with uncoated and coated HAP; **a**) neat PLA, **b**) uncoated, 0 wt% StAc, **c**) coated, 10 wt% StAc

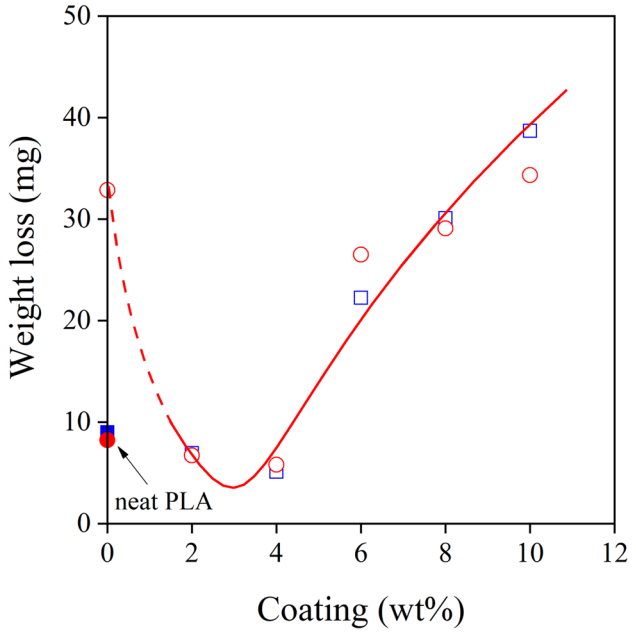

Fig. 4 The amount of PLA removed from the surface of neat PLA (full symbols) and PLA/HAP composites by enzymatic etching in 24 h determined by the direct measurement of weight (◯) or by complexation and UV-Vis spectrophotometry (□)

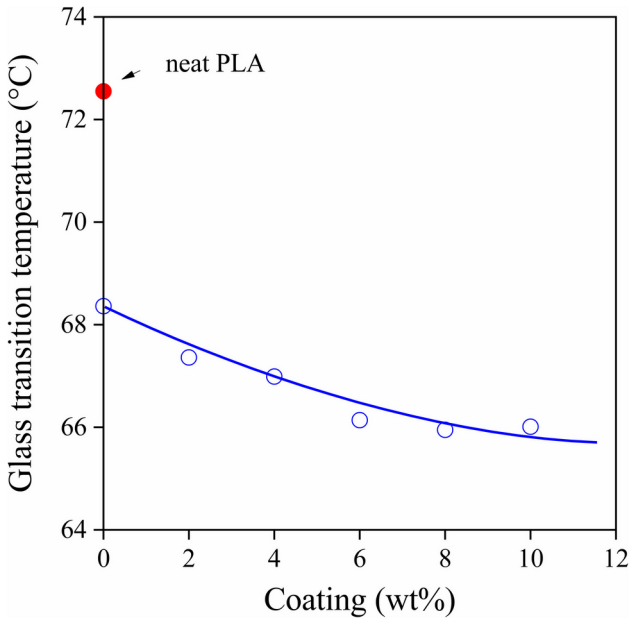

Fig. 5 Effect of the addition of HAP and surface modification on the glass transition temperature of PLA

strongly to the surface of HAP. The large value measured for the uncoated fillers is probably the effect of heterogeneous structure and increased molecular mobility [55]. The decrease at small StAc content, below monolayer coverage, must result from the more homogeneous structure compared to the polymer containing the uncoated hydroxyapatite. HAP particles are distributed more evenly in the polymer than large aggregates and they hinder the progress of degradation on the surface. The excess surfactant must modify the behavior of the polymer and probably increase the mobility of the polymer chains, which increases the probability of assuming conformations necessary for the interaction of the enzyme and PLA chains to exert the catalytic action of the former. Chain mobility in PLA was shown to increase upon the addition of basically any additive, including fillers and reinforcements [55], which can explain the relatively large difference between neat PLA and the uncoated HAP-containing sample. Small molecular weight components, like StAc, have a larger effect. Accordingly, increased mobility results in faster degradation and the removal of a thicker polymer layer from the surface. The tentative explanation is supported by the changing glass transition temperature (T_g) of the PLA matrix plotted against the extent of coating in Fig. 5. Glass transition temperature decreases already upon the addition of the uncoated HAP, which cannot be explained, in any other way, but increased mobility as reported earlier [55]. Surplus StAc decreases T_g further.

3.3 Characterization of the etched surface

The goal of etching is the removal of the surface polymer layer to disclose HAP and to modify the activity of the scaffold in cell adhesion and proliferation. The original and etched surfaces were studied by AFM. The surface of the neat polymer and the composite were smooth, without any characteristic features (Fig. 6a). Etching changed the surface completely. Higher regions (light) and pits (dark) could be observed both on the surface of the neat polymer and that of the composite containing HAP with 4 wt% StAc coating (Fig. 6b and c). The micrometer-sized white structural formations must be PLA crystallites. They are quite similar to those observed by others and interpreted as the crystalline phase of PLA [37]. It is difficult to distinguish the two surfaces in Fig. 6b and c, they seem to be very similar. Although contours are somewhat blurred at larger magnification, closer scrutiny reveals needle-like HAP crystals (highlighted by white circles in Fig. 6d), indicating that a large part of the mineral is distributed evenly as individual particles. Large aggregates cannot be seen on the surface at all showing that surface coating achieved its goal and the composite is homogeneous.

Further information is offered about the effect of etching on the surface morphology of the polymer and the composites by roughness. This latter quantity is plotted against the investigated area for selected materials in Fig. 7. Etching increased surface roughness considerably. Etched neat PLA has the roughest surface, which allows the drawing of several conclusions. The first is that enzymatic etching removes a considerable amount of PLA from the surface

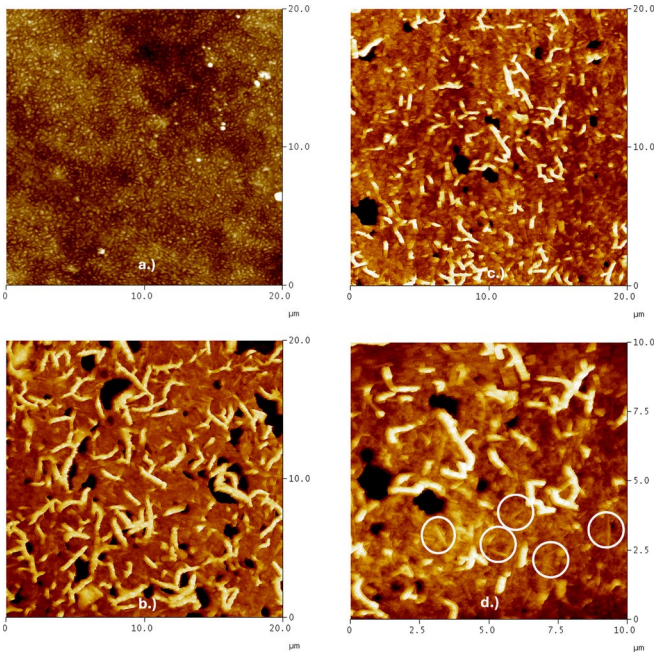

Fig. 6 AFM micrographs recorded on the surface of neat PLA and PLA/HAP composites. Effect of enzymatic etching. **a**) PLA/HAP (4 wt% StAc) before etching, **b**) neat PLA after etching, **c**) PLA/HAP (4 wt% StAc) after etching, **d**) PLA/HAP (4 wt% StAc) after etching, larger magnification showing individual HAP particles highlighted by white circles

(see roughness before etching). Etching proceeds unevenly, HAP particles hinder the progress of degradation, and they result in a more homogeneous, smoother surface. The thickness of the layer removed, estimated from weight loss, is around 4 μm for the sample with 10 wt% StAc coating, which should disclose HAP particles. The remaining question is the effect of coating on cell adhesion.

The measurement of surface energetics may offer further information about the presence or absence of HAP on the surface of the composites. The contact angle of water measured on the surface of the composites before and after etching is plotted against the extent of surface coating in Fig. 8. Contact angle is independent of coating before etching because all composites are covered by the PLA layer as discussed earlier. Etching changes surface energetics completely. The small contact angle measured on the composite containing the uncoated filler indicates that the latter has high energy and HAP is located on the surface resulting in

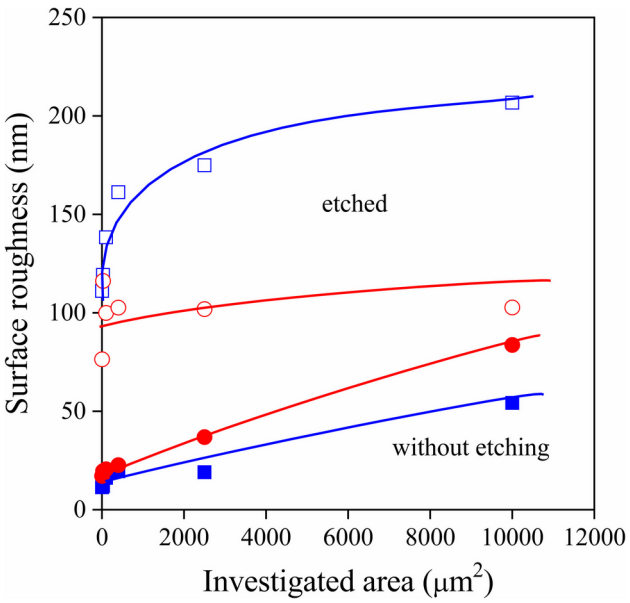

Fig. 7 Surface roughness of PLA and PLA/HAP samples plotted against the scanned area. Effect of coating and etching. Symbols: (■) neat PLA, (●) PLA/HAP (4 wt% StAc) without etching, (□) neat PLA after etching (◯) PLA/HAP (4 wt% StAc) after etching

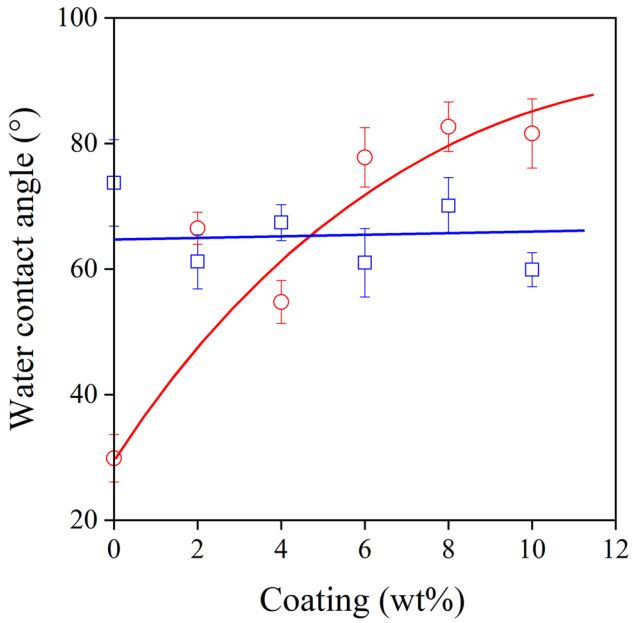

Fig. 8 Changes in the contact angle of water on the surface of PLA/HAP composites as an effect of surface coating and etching. Symbols: (□) before etching, (◯) after etching

strong interaction with water. Coating increases contact angle because of the appearance of the apolar stearic acid layer on the surface of HAP particles, and wettability decreases with increasing extent of coating. The question is the effect of this decreased polarity on the interaction with the cells.

The final proof for the presence of HAP particles on the surface and the beneficial effect of enzymatic etching is supplied by FTIR spectroscopy. The relevant region of spectra is compared in Fig. 9a for the neat HAP and for the composite containing HAP coated with 10 wt% StAc before and after etching. The intensity of the characteristic PO_4^{3-} vibration of HAP at 603 cm^{-1} [56] clearly increases as a result of etching. Although the quantitative evaluation of ATR spectra is difficult, the intensity of the characteristic band of HAP is plotted against the extent of coating before and after etching in Fig. 9b. The results clearly show that etching is efficient and brings HAP particles to the surface as intended, the intensity of the PO_4^{3-} vibration increased significantly as a result of etching. The results correlate well with the amount of removed PLA (Fig. 4).

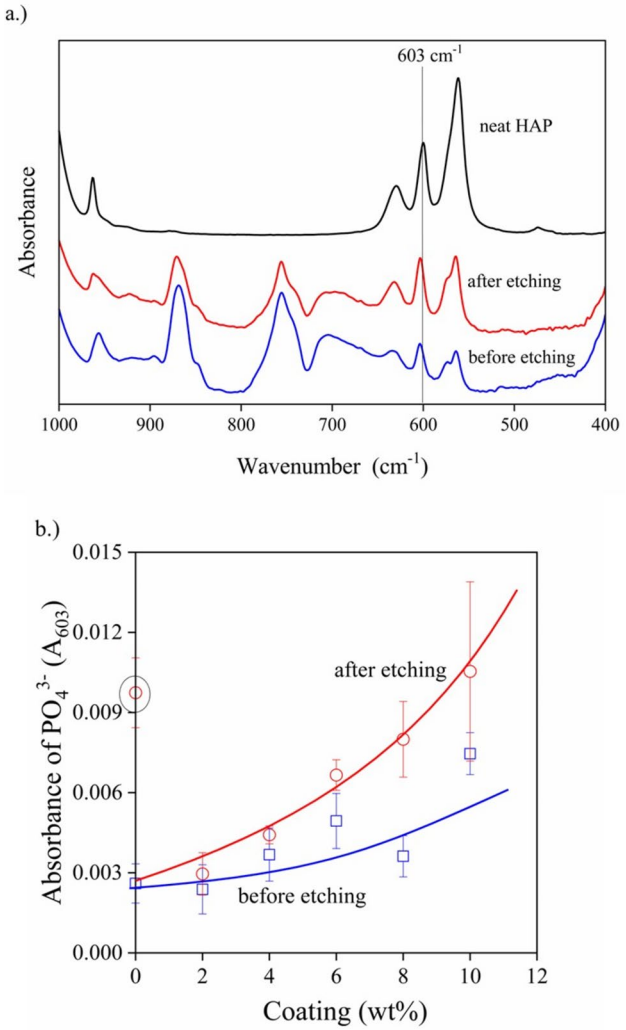

Fig. 9 Determination of the effect of etching on the surface composition of PLA/HAP composites by FTIR spectroscopy; **a**) the relevant region of the spectrum showing the characteristic PO_4^{3-} vibration of HAP, **b**) dependence of the intensity of the vibration on the extent of coating before (□) and after (◯) etching

3.4 Cell adhesion

The experiments were carried out according to the protocol described in the experimental part. The adhesion and survival of cells on the surface of the etched composites were studied as a function of the coating of HAP. Attached cells were detected by UV-Vis spectrophotometry after reaction with the XTT [2,3-bis(2-methoxy-4-nitro-5-sulfophenil)−2H-tetrazolium-5-carboxanilide] reagent. Living cells are colored orange, which makes possible their detection and quantitative determination. An optical micrograph recorded on the surface of neat PLA after the cell test is presented in Fig. 10a as an example. The cells represented by the orange areas are clearly visible in the micrograph.

Figure 8 shows that the surface of the scaffolds becomes apolar with increasing amount of coating, which might hinder the adhesion of cells to the surface. The micrographs were evaluated quantitatively, and optical density proportional to the amount of living cells is plotted against the extent of coating in Fig. 10b. Rather surprisingly, the extent of the coating does not influence the adhesion of the cells at all; thus, the composites containing surface coated HAP can be used for the preparation of scaffolds without endangering its interaction with the surrounding tissues. Cell differentiation and proliferation take a longer time, thus they must be studied at a later stage.

3.5 Discussion

The preparation of polymer/HAP scaffold materials may face several difficulties. The first is the proper dispersion of HAP in the polymer. The particles of the filler with high surface energy tend to aggregate, and aggregation becomes more extensive with decreasing particle size and increasing filler content. The best way to decrease the extent of aggregation is surface coating, the coverage of the surface with an amphiphilic organic compound to decrease surface energy. As the results of this study show, this approach is efficient but raises the question of changing interactions. As an effect of surface coating, all interactions change and not only particle/particle, but particle/matrix and particle/cell interactions as well.

The second problem is the inevitable formation of a polymer layer on the surface of all thermoplastic/HAP composites and the consequent isolation of growing cells from HAP, which is supposed to assist recovery. The results of

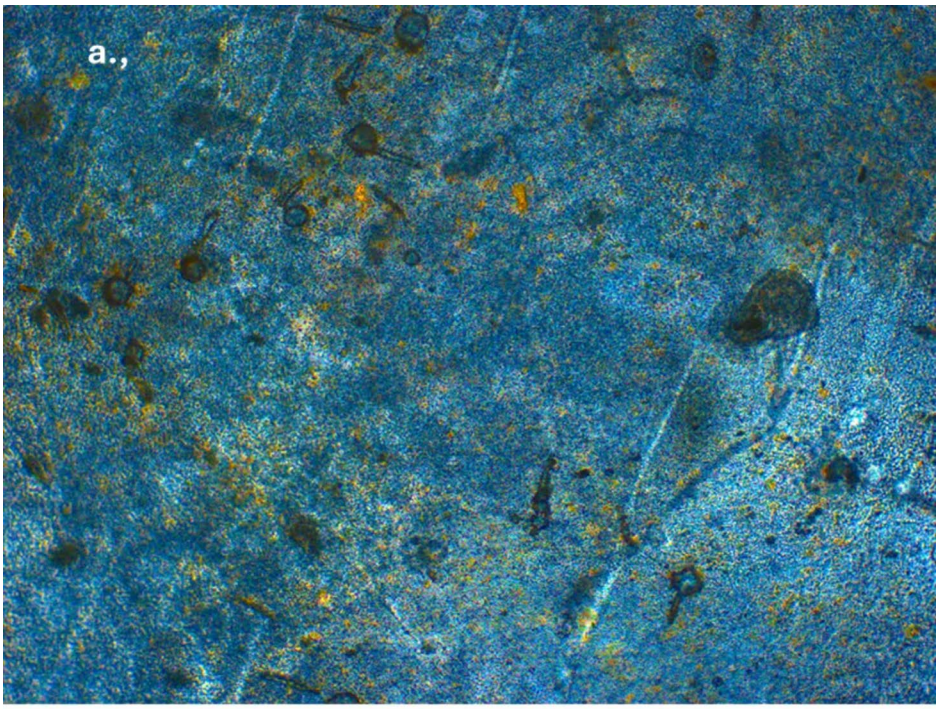

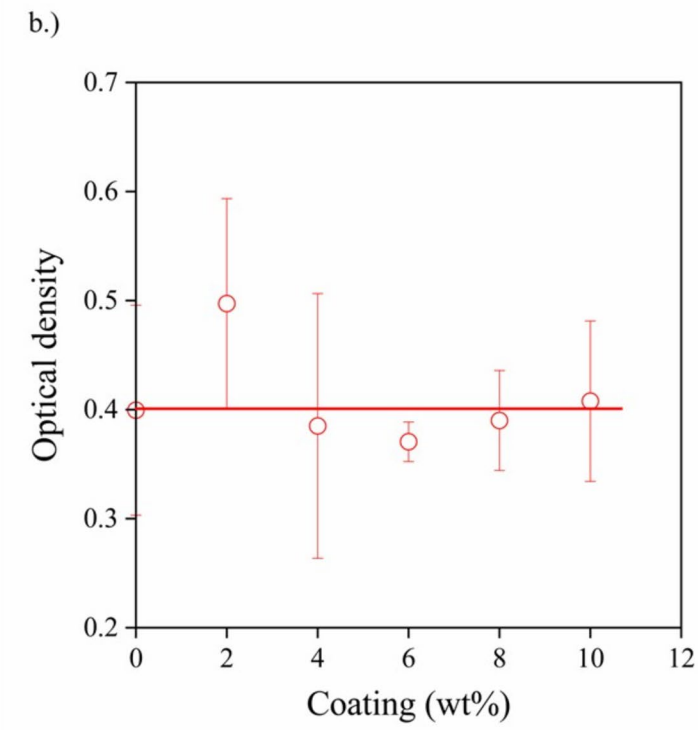

Fig. 10 Viability of cells on the surface of etched PLA and the effect of surface coating; **a**) optical micrograph recorded on the surface of neat PLA after the viability test, **b**) effect of stearic acid coating on optical density indicating the number of living cells

all experiments used for the characterization of the surface of the composites prepared [contact angle (Fig. 8), AFM (Fig. 6), FTIR (Fig. 9)] indicated that HAP particles are inherently absent from the surface of as prepared composites. Enzymatic etching removed a sufficiently thick layer from the surface of the composites thus disclosing HAP particles as shown by the same measurements. However, the etching of the surface does not solve the problem of changing surface energy and wettability as an effect of particle coating. Fortunately, the results of cell tests indicated that changing surface tension does not decrease adhesion (see Fig. 10b).

One remaining question that needs attention is the effect of the extent of surface coating on enzymatic degradation and the dependence of the amount of degraded material during etching, carried out under identical conditions. This amount changed according to a complicated function indicating the effect of several factors, including the presence of HAP particles, homogeneity, the changing surface characteristic of HAP, and surplus stearic acid. The amount of degraded material increases considerably after exceeding monolayer coverage, i.e. upon the appearance of surplus StAc. This surfactant increases the mobility of PLA molecules thus improving the efficiency of enzymatic degradation. Decreasing surface energy and surplus StAc increases mobility further (Fig. 5), thus assisting degradation; however, the increased homogeneity of nanoparticles has the opposite effect on the efficiency of the enzymatic degradation (Fig. 4). It is clear that a number of factors influence the structure and properties of PLA/HAP scaffolds, but the approach proposed here, i.e., surface modification and enzymatic etching, seems to solve some problems and lead to scaffolds that can be used in bone replacement more efficiently.

4 Conclusions

Nanosized HAP particles could be produced with the method used in this study. The small particles aggregated without surface modification. The application of stearic acid coating decreased aggregation and improved homogenization. The extent of coating must be optimized, the amount of stearic acid needed for monolayer coverage is around 4 wt% for the HAP prepared in this study. During the processing of PLA/HAP composites, a polymer layer forms on the surface of the product; HAP particles are not available to assist bone regeneration. The surface layer was removed successfully by enzymatic etching. The amount of removed PLA polymer depended quite strongly on the extent of the surface coating. Etching disclosed HAP particles leading to increased surface roughness and modified wettability. Disclosing surface-coated HAP particles resulted in decreased wettability, but this did not influence the adhesion of cells onto the surface. Scaffolds could be prepared successfully from the composites containing the coated particles by 3D printing, which, in all probability, can be successfully used for bone regeneration.

Acknowledgements The authors thank Bálint Dániel Fodor, Péter Tamás Németh, Soma Székhelyi and Rozemarie Nechifor for their technical assistance in the experiments. The authors are grateful to Alfréd Kallay-Menyhárd for his advice on the thermal measurements and Szilvia Klébert for the consultation on hydroxyapatite synthesis.

Author contributions Conceptualization: [Dóra Tátraaljai, Dorottya Kardos, Béla Pukánszky], Methodology: [István Hornyák, Románszki Loránd, Miroslav Slouf, János Móczó], Formal analysis and investigation: [Attila Ur, Dóra Plachi, Viktória Varga, Románszki Loránd, Miroslav Slouf, Nóra Hegyesi], Writing—original draft preparation: [Dóra Tátraaljai]; Writing—review and editing: [Béla Pukánszky], Funding acquisition: [Dóra Tátraaljai]; Resources: [Nóra Hegyesi]; Supervision: [Dóra Tátraaljai].

Funding Open access funding provided by HUN-REN Research Centre for Natural Sciences.
The research was supported by the University Research Fellowship Program (EKÖP-24-4-IIBME-163) and TKP2021-EGA funding scheme (Project no. TKP-9-8/PALY-2021) provided by the Ministry of Culture and Innovation of Hungary from the National Research, Development and Innovation Fund. Dóra Tátraaljai is grateful for the János Bolyai fellowship (BO/00596/24), provided by the Hungarian Academy of Sciences.

Data Availability The data that support the findings of this study are available from the corresponding author upon reasonable request.

Declarations

Competing interests The authors have no relevant financial or non-financial interests to disclose.

References

1. R. Vijayaraghavan, M. Vidyavathi, R.V. Suresh Kumar, S. Loganathan, R.B. Valapa, 3D bioprinted poly(lactic acid) scaffolds infused with curcumin-loaded nanostructured lipid carriers: a promising approach for skin regeneration. Biomater. Sci. **13**(5), 1286–1303 (2025). https://doi.org/10.1039/D4BM01550A
2. A. Oryan, S. Alidadi, A. Moshiri, Current concerns regarding healing of bone defects. Hard Tissue **2**(2), 1–12 (2013). https://doi.org/10.13172/2050-2303-2-2-374
3. A.R. Amini, C.T. Laurencin, S.P. Nukavarapu, Bone tissue engineering: recent advances and challenges. Crit. Rev.™ Biomed. Eng. **40**(5), 363–408 (2012). https://doi.org/10.1615/critrevbiomedeng.v40.i5.10
4. A.J. Salgado, O.P. Coutinho, R.L. Reis, Bone tissue engineering: state of the art and future trends. Macromol. Biosci. **4**(8), 743–765 (2004). https://doi.org/10.1002/mabi.200400026
5. K. Rezwan, Q. Chen, J.J. Blaker, A.R. Boccaccini, Biodegradable and bioactive porous polymer/inorganic composite scaffolds for bone tissue engineering. Biomaterials **27**(18), 3413–3431 (2006). https://doi.org/10.1016/j.biomaterials.2006.01.039

6. N. Goonoo, A. Bhaw-Luximon, D. Jhurry, Biodegradable polymer blends: miscibility, physicochemical properties and biological response of scaffolds. Polym. Int. **64**(10), 1289–1302 (2015). https://doi.org/10.1002/pi.4937
7. G. Wei, P.X. Ma, Structure and properties of nano-hydroxyapatite/polymer composite scaffolds for bone tissue engineering. Biomaterials **25**(19), 4749–4757 (2004). https://doi.org/10.1016/j.biomaterials.2003.12.005
8. L.M. Mathieu, T.L. Mueller, P.-E. Bourban, D.P. Pioletti, R. Müller, J.-A.E. Månson, Architecture and properties of anisotropic polymer composite scaffolds for bone tissue engineering. Biomaterials **27**(6), 905–916 (2006). https://doi.org/10.1016/j.biomaterials.2005.07.015
9. W. Wang, S. Liao, M. Liu, Q. Zhao, Y. Zhu, Polymer composites reinforced by nanotubes as scaffolds for tissue engineering. Int. J. Polym. Sci. **2014**(1), 805634 (2014). https://doi.org/10.1155/2014/805634
10. R. Karimi-Soflou, E. Mohseni-Vadeghani, A. Karkhaneh, Controlled release of resveratrol from a composite nanofibrous scaffold: effect of resveratrol on antioxidant activity and osteogenic differentiation. J. Biomed. Mater. Res. Part A **110**(1), 21–30 (2022). https://doi.org/10.1002/jbm.a.37262
11. J. Fernández, M. Ruiz-Ruiz, J.-R. Sarasua, Electrospun fibers of polyester, with both nano-and micron diameters, loaded with antioxidant for application as wound dressing or tissue engineered scaffolds. ACS Appl. Polym. Mater. **1**(5), 1096–1106 (2019). https://doi.org/10.1021/acsapm.9b00108
12. X. Liu, Y. Won, P.X. Ma, Surface modification of interconnected porous scaffolds. J. Biomed. Mater. Res. Part A: Off. J. Soc. Biomater. Jpn. Soc. Biomater. Aust. Soc. Biomater. Korean Soc. Biomater. **74**(1), 84–91 (2005). https://doi.org/10.1002/jbm.a.30367
13. N.R. Richbourg, N.A. Peppas, V.I. Sikavitsas, Tuning the biomimetic behavior of scaffolds for regenerative medicine through surface modifications. J. Tissue Eng. Regen. Med. **13**(8), 1275–1293 (2019). https://doi.org/10.1002/term.2859
14. A. Shanmugavadivu, N. Selvamurugan, Surface engineering of 3D-printed polylactic acid scaffolds with polydopamine and 4-methoxycinnamic acid–chitosan nanoparticles for bone regeneration. Nanoscale Adv. **7**(6), 1636–1649 (2025). https://doi.org/10.1039/D4NA00768A
15. A. Mehmood, N. Raina, V. Phakeenuya, B. Wonganu, K. Cheenkachorn, The current status and market trend of polylactic acid as biopolymer: awareness and needs for sustainable development. Mater. Today: Proc. **72**, 3049–3055 (2023). https://doi.org/10.1016/j.matpr.2022.08.387
16. N. Patel, D. Blumberga, Assessing biopolymer packaging in the EU market for sustainable bioeconomy development. Rigas Tehniskas Universitates Zinatniskie Raksti **28**(1), 342–355 (2024). https://doi.org/10.2478/rtuect-2024-0027
17. M. Penco, A. Rahman, S. Verstichel, B. De Wilde, P. Cinelli, A. Lazzeri, Biodegradable PLA/PC copolymers for automotive applications. Bioplastics **6**, 20–21 (2011)
18. K. Hamad, M. Kaseem, H. Yang, F. Deri, Y. Ko, Properties and medical applications of polylactic acid: a review. Express Polym. Lett. **9**(5), (2015). https://doi.org/10.3144/expresspolymlett.2015.42
19. T. Serra, M.A. Mateos-Timoneda, J.A. Planell, M. Navarro, 3D printed PLA-based scaffolds: a versatile tool in regenerative medicine. Organogenesis **9**(4), 239–244 (2013). https://doi.org/10.4161/org.26048
20. A. Grémare, V. Guduric, R. Bareille, V. Heroguez, S. Latour, N. L'heureux, J.C. Fricain, S. Catros, D. Le Nihouannen, Characterization of printed PLA scaffolds for bone tissue engineering. J. Biomed. Mater. Res. Part A **106**(4), 887–894 (2018). https://doi.org/10.1002/jbm.a.36289
21. A. Zimina, F. Senatov, R. Choudhary, E. Kolesnikov, N. Anisimova, M. Kiselevskiy, P. Orlova, N. Strukova, M. Generalova, V. Manskikh, Biocompatibility and physico-chemical properties of highly porous PLA/HA scaffolds for bone reconstruction. Polymers **12**(12), 2938 (2020). https://doi.org/10.3390/polym12122938
22. C.E. Corcione, F. Gervaso, F. Scalera, S.K. Padmanabhan, M. Madaghiele, F. Montagna, A. Sannino, A. Licciulli, A. Maffezzoli, Highly loaded hydroxyapatite microsphere/PLA porous scaffolds obtained by fused deposition modelling. Ceram. Int. **45**(2), 2803–2810 (2019). https://doi.org/10.1016/j.ceramint.2018.07.297
23. G. Dal Poggetto, U. D'Amora, A. Ronca, M.G. Raucci, A. Soriente, G. Gomez d'Ayala, P. Laurienzo, Chemical modification of PLA for the design of 3D printed nanocomposite scaffolds with enhanced degradability for bone tissue engineering. Polym. Compos. **n/a**(n/a), (2025). https://doi.org/10.1002/pc.29470
24. S. Sitthisang, X. Hou, A. Treetong, X. Xu, W. Liu, C. He, U. Saeed-Ueng, S. Yodmuang, Nanomechanical mapping of PLA hydroxyapatite composite scaffolds links surface homogeneity to stem cell differentiation. Sci. Rep. **14**(1), 21097 (2024). https://doi.org/10.1038/s41598-024-72073-z
25. J.O. Akindoyo, M.D. Beg, S. Ghazali, H.P. Heim, M. Feldmann, Impact modified PLA-hydroxyapatite composites–Thermo-mechanical properties. Compos. Part A: Appl. Sci. Manuf. **107**, 326–333 (2018). https://doi.org/10.1016/j.compositesa.2018.01.017
26. J.O. Akindoyo, M.D. Beg, S. Ghazali, H.P. Heim, M. Feldmann, Effects of surface modification on dispersion, mechanical, thermal and dynamic mechanical properties of injection molded PLA-hydroxyapatite composites. Compos. Part A: Appl. Sci. Manuf. **103**, 96–105 (2017). https://doi.org/10.1016/j.compositesa.2017.09.013
27. J. Li, X. Lu, Y. Zheng, Effect of surface modified hydroxyapatite on the tensile property improvement of HA/PLA composite. Appl. Surf. Sci. **255**(2), 494–497 (2008). https://doi.org/10.1016/j.apsusc.2008.06.067
28. S. Morelli, S. Salerno, J. Holopainen, M. Ritala, L. De Bartolo, Osteogenic and osteoclastogenic differentiation of co-cultured cells in polylactic acid–nanohydroxyapatite fiber scaffolds. J. Biotechnol. **204**, 53–62 (2015). https://doi.org/10.1016/j.jbiotec.2015.03.023
29. D. Yan, Z. Wang, Z. Guo, Y. Ma, C. Wang, H. Tan, Y. Zhang, Study on the properties of PLA/PBAT composite modified by nanohydroxyapatite. J. Market. Res. **9**(5), 11895–11904 (2020). https://doi.org/10.1016/j.jmrt.2020.08.062
30 A.M. Pandele, A. Constantinescu, I.C. Radu, F. Miculescu, S. IoanVoicu, L.T. Ciocan, Synthesis and characterization of PLA-Micro-structured hydroxyapatite composite films. Materials **13**(2), 274 (2020). https://doi.org/10.3390/ma13020274
31. G. Keledi, J. Hári, B. Pukánszky, Polymer nanocomposites: structure, interaction, and functionality. Nanoscale **4**(6), 1919–1938 (2012). https://doi.org/10.1039/C2NR11442A
32. U.V. Khomutova, A.G. Korzhova, A.A. Bryuzgina, O.A. Laput, I.V. Vasenina, Y.H. Akhmadeev, V.V. Shugurov, I.I. Azhazha, Y.G. Shapovalova, A.V. Chernyavskii, I.A. Kurzina, Nitrogen plasma treatment of composite materials based on polylactic acid and hydroxyapatite. Polymers **16**(5), 627 (2024). https://doi.org/10.3390/polym16050627
33. O. Laput, I. Vasenina, M.C. Salvadori, K. Savkin, D. Zuza, I. Kurzina, Low-temperature plasma treatment of polylactic acid and PLA/HA composite material. J. Mater. Sci. **54**(17), 11726–11738 (2019). https://doi.org/10.1007/s10853-019-03693-4
34. S. Klébert, S. Tilajka, L. Románszki, M. Mohai, E. Csiszár, Z. Károly, Degradation phenomena on atmospheric air plasma

treatment of polyester fabrics. Surf. Interfaces **22**, 100826 (2021). https://doi.org/10.1016/j.surfin.2020.100826
35. C. Guo, M.M. Xiang, Y.S. Dong, Surface modification of poly (lactic acid) with an improved alkali-acid hydrolysis method. Mater. Lett. **140**, 144–147 (2015). https://doi.org/10.1016/j.matlet.2014.10.099
36. L.L. Smith, P.J. Niziolek, K.M. Haberstroh, E.A. Nauman, T.J. Webster, Decreased fibroblast and increased osteoblast adhesion on nanostructured NaOH-etched PLGA scaffolds. Int. J. Nanomed. **2**(3), 383–388 (2007). https://doi.org/10.2147/IJN.S2.3.383
37. K. Numata, A. Finne-Wistrand, A.-C. Albertsson, Y. Doi, H. Abe, Enzymatic degradation of monolayer for poly (lactide) revealed by real-time atomic force microscopy: effects of stereochemical structure, molecular weight, and molecular branches on hydrolysis rates. Biomacromolecules **9**(8), 2180–2185 (2008). https://doi.org/10.1021/bm800281d
38. N.F. Zaaba, M. Jaafar, A review on degradation mechanisms of polylactic acid: hydrolytic, photodegradative, microbial, and enzymatic degradation. Polym. Eng. Sci. **60**(9), 2061–2075 (2020). https://doi.org/10.1002/pen.25511
39. A. Shalem, O. Yehezkeli, A. Fishman, Enzymatic degradation of polylactic acid (PLA). Appl. Microbiol. Biotechnol. **108**(1), 413 (2024). https://doi.org/10.1007/s00253-024-13212-4
40. R. Donate, M. Monzón, M.E. Alemán-Domínguez, Z. Ortega, Enzymatic degradation study of PLA-based composite scaffolds. Rev. Adv. Mater. Sci. **59**(1), 170–175 (2020). https://doi.org/10.1515/rams-2020-0005
41. S. György, Z. Károly, P. Fazekas, P. Németh, E. Bódis, A. Menyhárd, L. Kótai, S. Klébert, Effect of the reaction temperature on the morphology of nanosized HAp. J. Therm. Anal. Calorim. **138**(1), 145–151 (2019). https://doi.org/10.1007/s10973-019-08255-z
42. M. Zhang, A.-J. Wang, J.-M. Li, N. Song, Effect of stearic acid modified HAp nanoparticles in different solvents on the properties of Pickering emulsions and HAp/PLLA composites. Mater. Sci. Eng.: C **79**, 255–261 (2017). https://doi.org/10.1016/j.msec.2017.05.045
43. L. Borshchevskaya, T. Gordeeva, A. Kalinina, S. Sineokii, Spectrophotometric determination of lactic acid. J. Anal. Chem. **71**, 755–758 (2016). https://doi.org/10.1134/S1061934816080037
44. J.L. Lábár, M. Adamik, B. Barna, Z. Czigány, Z. Fogarassy, Z.E. Horváth, O. Geszti, F. Misják, J. Morgiel, G. Radnóczi, Electron diffraction based analysis of phase fractions and texture in nanocrystalline thin films, part III: application examples. Microsc. Microanal. **18**(2), 406–420 (2012). https://doi.org/10.1017/s1431927611012803
45. W. Kraus, G. Nolze, POWDER CELL–a program for the representation and manipulation of crystal structures and calculation of the resulting X-ray powder patterns. J. Appl. Crystallogr. **29**(3), 301–303 (1996). https://doi.org/10.1107/S0021889895014920
46 M. Naderi, Surface area: Brunauer–Emmett–Teller (BET), in *Progress in Filtration and Separation*. (Elsevier, 2015), pp.585–608
47. U. Kostiv, O. Janoušková, M. Šlouf, N. Kotov, H. Engstová, K. Smolková, P. Ježek, D. Horák, Silica-modified monodisperse hexagonal lanthanide nanocrystals: synthesis and biological properties. Nanoscale **7**(43), 18096–18104 (2015). https://doi.org/10.1039/C5NR05572E
48 L. Ondrák, K. OndrákFialová, M. Sakmár, M. Vlk, K. Štamberg, B. Drtinová, M. Šlouf, F. Bruchertseifer, A. Morgenstern, J. Kozempel, Preparation and characterization of α-zirconium phosphate as a perspective material for separation of 225Ac and 213Bi. J. Radioanal. Nucl. Chem. **332**(5), 1475–1481 (2023). https://doi.org/10.1007/s10967-022-08682-7
49. J. Cé de Andrade, F. Cabral, F.J. Clemens, J. Leite Vieira, M.B.P. Soares, D. Hotza, M.C. Fredel, Effect of stearic acid on the mechanical and rheological properties of PLA/HA biocomposites. Mater. Today Commun. **35**, 106357 (2023). https://doi.org/10.1016/j.mtcomm.2023.106357
50. Y. Li, W. Weng, Surface modification of hydroxyapatite by stearic acid: characterization and in vitro behaviors. J. Mater. Sci. - Mater. Med. **19**, 19–25 (2008). https://doi.org/10.1007/s10856-007-3123-5
51. J. Móczó, B. Pukánszky, Polymer micro and nanocomposites: structure, interactions, properties. J. Ind. Eng. Chem. **14**(5), 535–563 (2008). https://doi.org/10.1016/j.jiec.2008.06.011
52. F. Kádár, L. Százdi, E. Fekete, B. Pukánszky, Surface characteristics of layered silicates: influence on the properties of clay/polymer nanocomposites. Langmuir **22**(18), 7848–7854 (2006). https://doi.org/10.1021/la060144c
53. D.N. Bikiaris, Nanocomposites of aliphatic polyesters: An overview of the effect of different nanofillers on enzymatic hydrolysis and biodegradation of polyesters. Polym. Degrad. Stab. **98**(9), 1908–1928 (2013). https://doi.org/10.1016/j.polymdegradstab.2013.05.016
54. N. Hegyesi, Y. Zhang, A. Kohári, P. Polyák, X. Sui, B. Pukánszky, Enzymatic degradation of PLA/cellulose nanocrystal composites. Ind. Crops Prod. **141**, 111799 (2019). https://doi.org/10.1016/j.indcrop.2019.111799
55. P. Müller, B. Imre, J. Bere, J. Móczó, B. Pukánszky, Physical ageing and molecular mobility in PLA blends and composites. J. Therm. Anal. Calorim. **122**, 1423–1433 (2015). https://doi.org/10.1007/s10973-015-4831-6
56. C. Chappard, G. André, M. Daudon, D. Bazin, Analysis of hydroxyapatite crystallites in subchondral bone by Fourier transform infrared spectroscopy and powder neutron diffraction methods. C. R. Chim. **19**(11), 1625–1630 (2016). https://doi.org/10.1016/j.crci.2015.03.015